

Imprints of high-density nuclear symmetry energy on the crustal fraction of neutron star moment of inertia *

Nai-Bo ZHANG¹ Bao-An Li²

¹ Shandong Provincial Key Laboratory of Optical Astronomy and Solar-Terrestrial Environment, School of Space Science and Physics, Institute of Space Sciences, Shandong University, Weihai, 264209, China

² Department of Physics and Astronomy, Texas A&M University-Commerce, Commerce, TX 75429-3011, USA

Abstract: The density dependence of nuclear symmetry energy $E_{\text{sym}}(\rho)$ remains the most uncertain aspect of the equation of state (EOS) of supradense neutron-rich nucleonic matter. Implications of observational crustal fraction of neutron star (NS) moment of inertia $\Delta I/I$ on the $E_{\text{sym}}(\rho)$ are examined in the present work, utilizing an isospin-dependent parameterization of NS EOS. We find that symmetry energy parameters significantly influence the $\Delta I/I$, while the EOS of symmetric nuclear matter has a negligible effect. An increase in the slope L and skewness J_{sym} of symmetry energy results in a larger $\Delta I/I$, whereas an increase in the curvature K_{sym} leads to a reduction in $\Delta I/I$. Additionally, we discuss the imprints of observational $\Delta I/I$ on the symmetry energy for NSs with masses of $1.0 M_{\odot}$ or $1.4 M_{\odot}$. Our results indicate that the $\Delta I/I$ has the potential to set a lower limit of symmetry energy at densities exceeding $3\rho_0$, particularly when L is constrained to values less than 60 MeV, thereby enhancing our understanding of supradense NS matter.

Key words: neutron stars, symmetry energy, moment of inertia

PACS: 97.60.Jd, 26.60.+c, 04.30.-w

1 Introduction

The Equation of State (EOS) of neutron-rich matter plays a crucial role in determining many properties of neutron stars (NSs). Unfortunately, it still has significant uncertainties especially at high densities. The high-density behavior of nuclear symmetry energy E_{sym} has long been recognized as the most uncertain aspect of the EOS of supradense neutron-rich nucleonic matter. This uncertainty stems from our limited understanding of the weak isospin-dependence of the strong force, the spin-isospin dependence of three-body nuclear forces, and the tensor-force-induced isospin-dependence of short range nucleon-nucleon correlations in dense matter, compounded by the challenges of accurately solving nuclear many-body problems [1]. The symmetry energy significantly influences various properties of neutron stars, including their radii, deformations and polarizabilities, moments of inertia, and the crust-core transition density [2, 3]. Thus, constraining the EOS or E_{sym} remains a

critical question for both the nuclear physics and astrophysics communities [4–9].

Fortunately, terrestrial nuclear experiments and astrophysical observations have provided tighter constraints over the past decades. For example, the mass of the most massive NS observed so far, e.g., the mass of PSR J0740+6620 has recently been updated to $2.08 \pm 0.07 M_{\odot}$ [10, 11], with its radius constrained to $R = 13.7_{-1.5}^{+2.6}$ km [12] or $R = 12.39_{-0.98}^{+1.30}$ km [13] by the Neutron Star Interior Composition Explorer (NICER) Collaboration. Additionally, with a significant increase in the dataset, updated analyses of the radius have been reported in Refs. [14–16]. Furthermore, the tidal deformability of neutron star with $1.4 M_{\odot}$ (canonical neutron star) has been extracted from the binary neutron star merger event GW170817, yielding $80 < \Lambda_{1.4} < 580$ at the 90% confidence level, as reported by the LIGO and Virgo Collaborations [17]. Although these observations still carry substantial uncertainties, they have been repeatedly employed in various analyses to enhance our understanding

Received *** 2024

* BAL is supported in part by the U.S. Department of Energy, Office of Science, under Award Number DE-SC0013702, the CUSTIPEN (China-U.S. Theory Institute for Physics with Exotic Nuclei) under the US Department of Energy Grant No. DE-SC0009971. NBZ is supported in part by the National Natural Science Foundation of China under Grant No. 12375120, the Zhishan Young Scholar of Southeast University under Grant No. 2242024RCB0013 and the Start-up Research Fund of Southeast University under Grant No. RF1028623060.

1) E-mail: naibo Zhang@seu.edu.cn

2) E-mail: Bao-An.Li@tamuc.edu

©2013 Chinese Physical Society and the Institute of High Energy Physics of the Chinese Academy of Sciences and the Institute of Modern Physics of the Chinese Academy of Sciences and IOP Publishing Ltd

of neutron star matter (see, e.g., Refs. [18–20] for reviews).

In addition to the aforementioned observational data, the glitch phenomenon in pulsars can also serve to constrain the EOS or E_{sym} [21–25]. This phenomenon, characterized by sudden increases in spin frequency, was first observed in the Vela pulsar [26, 27] and has since been detected in approximately 6% of all known pulsars. Glitches occur due to the transfer of angular momentum from the superfluid component of the stellar interior to the solid crust [28–30]. Previous studies have indicated that the glitch phenomenon is closely associated with the crustal fraction of the moment of inertia $\Delta I/I$, where I represents the total moment of inertia of the star and ΔI is the moment of inertia of the crust. By combining glitch data from the Vela pulsar and six other pulsars, Ref. [31] established that $\Delta I/I$ in a neutron star must exceed 1.4%. Notably, this constraint does not depend on the mass of the neutron star, leading many references to assume masses of either $1.0 M_{\odot}$ or $1.4 M_{\odot}$, resulting in conditions of $(\Delta I/I)_{1.4} \geq 1.0\%$ or $(\Delta I/I)_{1.4} \geq 1.4\%$. This lower limit was later increased to 1.6% [32]. While this limit can be met by nearly all EOSs, accounting for the entrainment of superfluid neutrons in the crust raises the constraint to $\Delta I/I \geq 7\%$ [33, 34], providing a more stringent condition for constraining the EOS or E_{sym} .

In our previous study [35], we simultaneously considered the maximum observed mass of PSR J0740+6620, the simultaneous measurement of mass and radius for this pulsar, and the tidal deformability from GW170817 to extract constraints on the EOS and E_{sym} . We found that the E_{sym} at densities greater than $3\rho_0$ still exhibits significant uncertainties, highlighting the need for additional observational data. In this work, we examine prospects of using the crustal fraction of NS moment of inertia $\Delta I/I$ to constrain the EOS and especially E_{sym} at suprasaturation densities using an isospin-dependent parameterization for the EOS of NS matter. We find that symmetry energy parameters significantly influence the $\Delta I/I$, while the EOS of symmetric nuclear matter has a negligible effect. An increase in the slope L and skewness J_{sym} of symmetry energy results in a larger $\Delta I/I$, whereas an increase of its curvature K_{sym} leads to a reduction in $\Delta I/I$.

The remainder of the paper is organized as follows: in the next section, we introduce the meta-model EOSs describing nuclear matter and detail the calculations of $\Delta I/I$ and NS crust-core transition properties. Section III discusses symmetry energy effects on the crustal fraction of NS moment of inertia. Finally, we summarize our findings in Section IV.

2 Theoretical framework

2.1 Explicitly isospin-dependent meta-model EOS for super-dense neutron-rich nuclear matter

A meta-model is a model of models. In the present work, we assume the neutron star matter is made of neutron-rich nuclear matter ($npe\mu$) at β -equilibrium described by a meta-model constructed in Ref. [36]. The energy density for $npe\mu$ matter at β -equilibrium can be calculated from

$$\varepsilon(\rho, \delta) = \rho[E(\rho, \delta) + M_N] + \varepsilon_l(\rho, \delta), \quad (1)$$

where the first term donates the energy density of nucleons and $\varepsilon_l(\rho, \delta)$ denotes the energy density for leptons (electrons and muons) that can be calculated from, e.g., the noninteracting Fermi gas model [37]. $\delta = (\rho_n + \rho_p)/\rho$ is the isospin asymmetry, M_N represents the average nucleon mass of 938 MeV, and $E(\rho, \delta)$ is the EOS of asymmetric nuclear matter which is a parabolic function of δ [38]:

$$E(\rho, \delta) = E_0(\rho) + E_{\text{sym}}(\rho) \cdot \delta^2 + \mathcal{O}(\delta^4), \quad (2)$$

where $E_0(\rho)$ is the EOS of symmetric nuclear matter (SNM) and $E_{\text{sym}}(\rho)$ is nuclear symmetry energy at density ρ . Once the energy density is determined, the baryon densities ρ_i of particle i can be obtained by solving the β -equilibrium condition $\mu_n - \mu_p = \mu_e = \mu_{\mu} \approx 4\delta E_{\text{sym}}(\rho)$ where $\mu_i = \partial\varepsilon(\rho, \delta)/\partial\rho_i$ and charge neutrality condition $\rho_p = \rho_e + \rho_{\mu}$. The pressure of neutron-rich nuclear matter can be calculated from

$$P(\rho) = \rho^2 \frac{d\varepsilon(\rho, \delta(\rho))/\rho}{d\rho}. \quad (3)$$

Then a EOS is obtained. To generate a series of EOSs with continuously variable parameters, we parameterize the $E_0(\rho)$ and $E_{\text{sym}}(\rho)$ as

$$E_0(\rho) = E_0(\rho_0) + \frac{K_0}{2} \left(\frac{\rho - \rho_0}{3\rho_0}\right)^2 + \frac{J_0}{6} \left(\frac{\rho - \rho_0}{3\rho_0}\right)^3, \quad (4)$$

$$\begin{aligned} E_{\text{sym}}(\rho) &= E_{\text{sym}}(\rho_0) + L \left(\frac{\rho - \rho_0}{3\rho_0}\right) \\ &+ \frac{K_{\text{sym}}}{2} \left(\frac{\rho - \rho_0}{3\rho_0}\right)^2 + \frac{J_{\text{sym}}}{6} \left(\frac{\rho - \rho_0}{3\rho_0}\right)^3. \end{aligned} \quad (5)$$

More details about this model can be found in our previous publications [35, 39–45].

Based on the accumulations of terrestrial nuclear experiment and astrophysical observations in past decades, the binding energy $E_0(\rho_0)$ and incompressibility K_0 of SNM at the saturation density have been tightly constrained to $E_0(\rho_0) = -15.9 \pm 0.4$ MeV and $K_0 = 240 \pm 20$

MeV [46, 47]. Based on surveys of 53 analyses of different kinds of terrestrial and astrophysical data available up to 2016 October, the magnitude $E_{\text{sym}}(\rho_0)$ and slope L of symmetry energy at ρ_0 are constrained to $E_{\text{sym}}(\rho_0) = 31.7 \pm 3.2$ MeV and $L = 58.7 \pm 28.1$ MeV [7, 48], respectively. For the parameters characterizing the medium- or high-density behavior of neutron-rich nuclear matter, the curvature of the symmetry energy is around $K_{\text{sym}} = -100 \pm 100$ MeV [20, 49–52], while the skewness of the SNM EOS is constrained to $J_0 = -190 \pm 100$ MeV [53–55] based on terrestrial experiments and astrophysical observations. Few constraints on J_{sym} have been obtained so far, and it is only very roughly known to be around $-200 < J_{\text{sym}} < 800$ MeV [56–58]. However, as small J_{sym} leads to low mass neutron stars, especially when J_{sym} is negative, we choose the lower boundary of J_{sym} as 200 MeV in the present work. We emphasize that the above parameters can be varied independently within their uncertain ranges given above. In fact, some of the uncertainty ranges are obtained from the marginalized posterior probability distribution functions (PDFs) of individual parameters in Bayesian analyses of NS observables. Nevertheless, once new observables or physics conditions are considered, correlations among the updated posterior EOS parameters may be introduced. In this work, however, all EOS parameters should be considered independent in their current uncertainty ranges given above.

Compared with EOSs from microscopic and/or phenomenological nuclear many-body theories, as well as piecewise polytropes or spectrum functions, here we want to emphasize the following aspects of the meta-model and justifications for using it. First of all, for microscopic and/or phenomenological nuclear many-body theories of neutron star matter, though numerous fundamental physical details can be included, it is challenging to isolate the individual effects of each parameter on the properties of neutron stars as they are typically exhibit correlations. On the contrary, all parameters of our meta-model can be varied independently within their presently known uncertainties. In addition, the meta-model can generate different EOSs that can mimic essentially all existing EOSs predicted by basically all microscopic and/or phenomenological theories by varying the meta-model EOS parameters. Secondly, we emphasize here that our model is different from the Taylor expansions where the convergence problem arise for densities larger than about $1.5\rho_0$. In fact, the parameterizations given by Eqs. (4) and (5) have dual meanings. On one hand, as parameterizations, mathematically they can be valid at any density without the convergence issue even at $(2-3)\rho_0$ and beyond. Their parameters can be extracted from astrophysical observations or terrestrial experiments. On the other hand, when approach-

ing the saturation density, the Eqs. (4) and (5) are exact the Taylor expansions up to the third order. More detailed demonstrations can be found in our previous work [36, 39, 44].

At densities below the crust-core transition point, we choose the Negele-Vautherin (NV) EOS [59] for the inner crust and the Baym-Pethick-Sutherland (BPS) EOS [60] for the outer crust. Once the parameters in Eqs. (4) and (5) are fixed and the transition density is calculated, a unique EOS is obtained and the properties, such as, mass and radius, can be calculated by solving the TOV equations [37, 61].

2.2 Crustal fraction of moment of inertia

In the present work, as we want to check how the observation of crustal fraction of the moment of inertia $\Delta I/I$ can constrain the parameters shown in Eqs. (4) and (5), we calculate the $\Delta I/I$ using the following formalism given in Ref. [31],

$$\frac{\Delta I}{I} = \frac{28\pi P_t R^3}{3Mc^2} \frac{(1 - 1.67\xi - 0.6\xi^2)}{\xi} \times \left[1 + \frac{2P_t}{\rho_t m_b c^2} \frac{1 + 5\xi - 14\xi^2}{\xi^2} \right], \quad (6)$$

where $\xi = GM/Rc^2$ is the dimensionless compactness, and $m_b = 930$ MeV/c² is the mass of ¹²C/12 or ⁵⁶Fe/56 [2, 3].

As shown in the above equation, the crustal fraction of moment of inertia of neutron star is quite sensitive to the crust-core transition density ρ_t and the pressure P_t there. The crust-core transition density ρ_t can be found by examining when the incompressibility of NS matter in the uniform core vanishes [62–64]

$$K_\mu = \rho^2 \frac{d^2 E_0}{d\rho^2} + 2\rho \frac{dE_0}{d\rho} + \delta^2 \times \left[\rho^2 \frac{d^2 E_{\text{sym}}}{d\rho^2} + 2\rho \frac{dE_{\text{sym}}}{d\rho} - 2E_{\text{sym}}^{-1} \left(\rho \frac{dE_0}{d\rho} \right)^2 \right] = 0. \quad (7)$$

Once K_μ becomes negative, the speed of sound becomes imaginary. It indicates the onset of the mechanical instability (spinodal decomposition of matter) in the core, leading to the formation of clusters making up the crust. This method has been used extensively in the literature to locate the crust-core transition point using various EOSs (see, e.g., [65–68]). As the E_{sym} and E_0 appear explicitly in the above equation, it is thus necessary and interesting to explore whether E_{sym} and E_0 have significant effects on the crustal fraction of NS moment of inertia [69, 70]. The flexibility of the meta-model and the very diverse EOSs generated with it enable us to explore

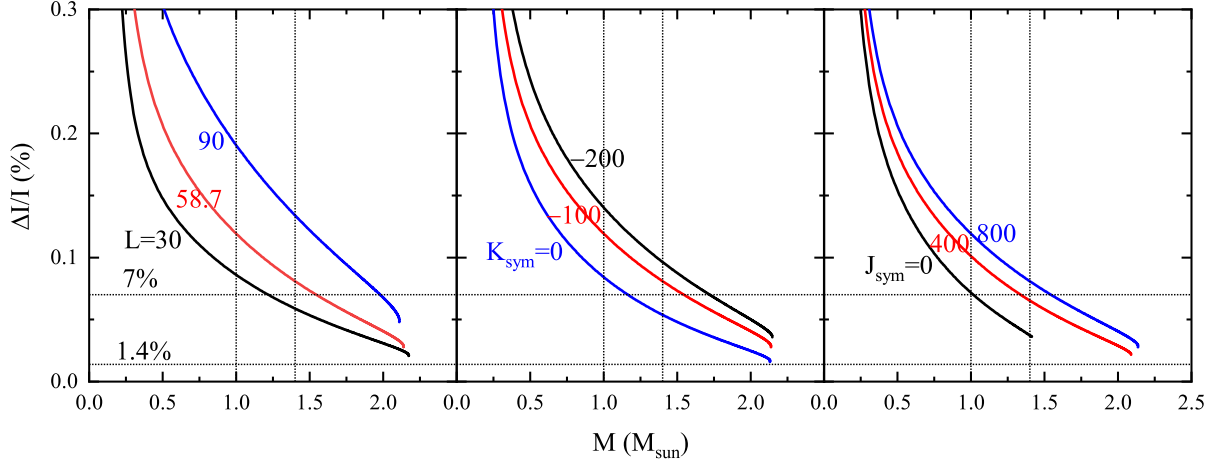


Fig. 1. The effects of the slope L (left panel), curvature K_{sym} (middle panel), and skewness J_{sym} (right panel) of symmetry energy on the crustal fraction of NS moment of inertia $\Delta I/I$. The horizontal dotted lines represent the constraints of 1.4% and 7%, while the vertical dotted lines correspond to neutron star masses of 1.0 and 1.4 M_{\odot} .

possible effects of E_{sym} and E_0 on $\Delta I/I$ more easily and broadly. In particular, we focus on effects of the high-order coefficients of nuclear symmetry energy (K_{sym} and J_{sym}) that have not been studied yet in the literature. Since the crust-core transition density and pressure are determined by the curvature of NS matter in Eq. (7), the K_{sym} and J_{sym} are expected to be important for determining the $\Delta I/I$.

3 Results and discussions

3.1 Effects of nuclear EOS parameters on the crustal fraction of NS moment of inertia

Effects of the slope L (left panel), curvature K_{sym} (middle panel), and skewness J_{sym} (right panel) of nuclear symmetry energy on the crustal fraction of NS moment of inertia $\Delta I/I$ are illustrated in Fig. 1. The horizontal dotted lines represent the constraints of 1.4% and 7%, while the vertical dotted lines correspond to neutron star masses of 1.0 and 1.4 M_{\odot} . Other parameters are kept at their most probable values currently known as previously mentioned. From the figure, it is evident that the symmetry energy parameters exert minimal influence on the NS maximum mass reached, with the exception of $J_{\text{sym}} = 0$, which results in a very soft EOS at high densities. Additionally, all symmetry energy parameters significantly affect the crustal fraction of NS moment of inertia. More specifically, as L increases, the $\Delta I/I$ consistently increases for a given NS mass. The condition $\Delta I/I > 1.4\%$ is easily satisfied, whereas $\Delta I/I > 7\%$ is only met when $M < 1.21 M_{\odot}$ for $L = 30$ MeV and $M < 1.98 M_{\odot}$ for $L = 90$ MeV, respectively. This indicates that the constraint of $\Delta I/I > 7\%$ can exclude $L = 30$ MeV for neutron stars with masses larger than 1.21 M_{\odot} , while favoring larger values of L that allow for a

broader mass range to satisfy the $\Delta I/I > 7\%$ constraint.

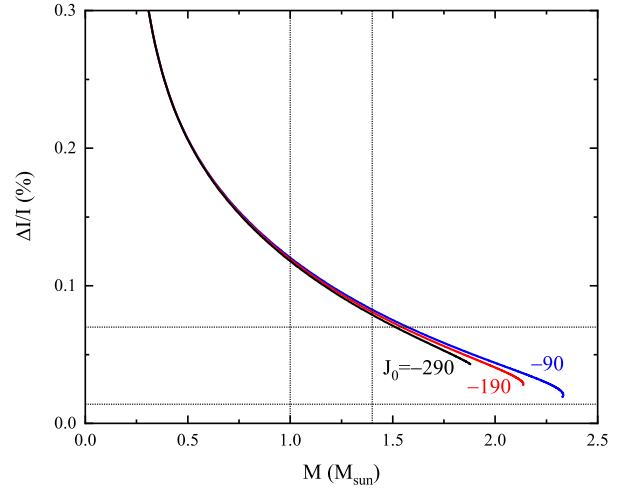


Fig. 2. (color online) Same as Fig. 1 but for the skewness J_0 of SNM.

A similar trend is observed for K_{sym} and J_{sym} . However, an increase in K_{sym} leads to a decrease in $\Delta I/I$. This is due to the fact that a higher K_{sym} results in a lower crust-core transition density, particularly affecting the transition pressure. On the other hand, an increase in L or J_{sym} raises the crust-core transition density, as shown in Fig. 3 of Ref. [36]. It is important to note that since the symmetry energy at saturation density is well constrained, the effects of $E_{\text{sym}}(\rho_0)$ are not significant and are thus not depicted here. Consequently, the competition among the symmetry energy parameters ultimately determines the value of $\Delta I/I$ and its mass dependence.

In addition to the effects of nuclear symmetry energy, effects of the skewness J_0 of the SNM on the crustal

fraction of NS moment of inertia $\Delta I/I$ are illustrated in Fig.2. It is seen that J_0 has minimal impact on $\Delta I/I$, leading us to fix $J_0 = -190$ MeV in the subsequent discussions regarding $\Delta I/I$. However, J_0 does significantly influence the maximum mass of neutron stars, which increases from 1.88 to 2.33 M_\odot as J_0 rises from -290 MeV to -90 MeV. Similar findings have been reported in our previous publications (e.g., Refs.[36, 39, 40]). Likewise, effects of the incompressibility K_0 of SNM are not shown here, as it is well constrained and has little effect on the $\Delta I/I$.

Based on the discussions above, we conclude that while the symmetry energy can significantly affect the moment of inertia, the EOS of SNM has minimal impact. Thus, we will focus on the effects of symmetry energy in the following subsection.

3.2 Constraints on symmetry energy parameters imposed by crustal fraction of NS moment of inertia

Currently, the highest mass of observed NSs is around 1.0 M_\odot , while most of NSs have masses around 1.4 M_\odot . For the integrity of following discussions, both NSs with mass of 1.0 M_\odot and 1.4 M_\odot are included.

Fixing the lower mass limit of neutron stars at 1.0 M_\odot , Fig. 3 presents the contour of the crustal fraction of NS moment of inertia $\Delta I/I$ in the K_{sym} and J_{sym} plane for slope of symmetry energy $L = 30$ MeV (upper panel), 60 MeV (middle panel), and 90 MeV (lower panel), respectively. The red lines indicate the constraint of $\Delta I/I = 7\%$. It is apparent that $\Delta I/I \geq 7\%$ or 1.4% can be satisfied for all values of L considered. The maximum $\Delta I/I$ appears at $K_{\text{sym}} = -200$ and $J_{\text{sym}} = 800$ MeV, as previously shown in Fig. 1, $\Delta I/I$ increases with increasing J_{sym} but decreases with K_{sym} . Additionally, the allowed range expands as L increases.

For $L = 30$ MeV, the area below the red line is excluded. Although the individual uncertainties in K_{sym} and J_{sym} cannot be narrowed further compared to their initial uncertainties, the combinations of these parameters are significantly constrained. In other words, nearly half of the parameter plane is excluded, particularly when both K_{sym} and J_{sym} are small. Furthermore, the relationship between K_{sym} and J_{sym} for constant $\Delta I/I$ is not monotonic. As K_{sym} increases, the curves for fixed $\Delta I/I$ initially rise and then fall. At $K_{\text{sym}} = -200$ MeV, J_{sym} must exceed 294 MeV, which can be explained by examining the transition density and pressure, as discussed below.

For $L = 60$ MeV, the relationship between K_{sym} and J_{sym} for constant $\Delta I/I$ becomes monotonic, and the lower right region of the plane is excluded. The upper limit of K_{sym} is constrained to be 41 MeV, while J_{sym} remains unconstrained for $L = 60$ MeV. Thus, the crustal

fraction of NS moment of inertia can help constrain the symmetry energy at medium densities characterized by K_{sym} , rather than at high densities, for larger values of L . When L increases to 90 MeV, only a negligible range is excluded to satisfy $\Delta I/I \geq 7\%$ in the lower right corner. Given that the upper limit of K_{sym} is constrained to be about 0, symmetry energies with larger values of L cannot be constrained at any density by the $\Delta I/I \geq 7\%$ constraint.

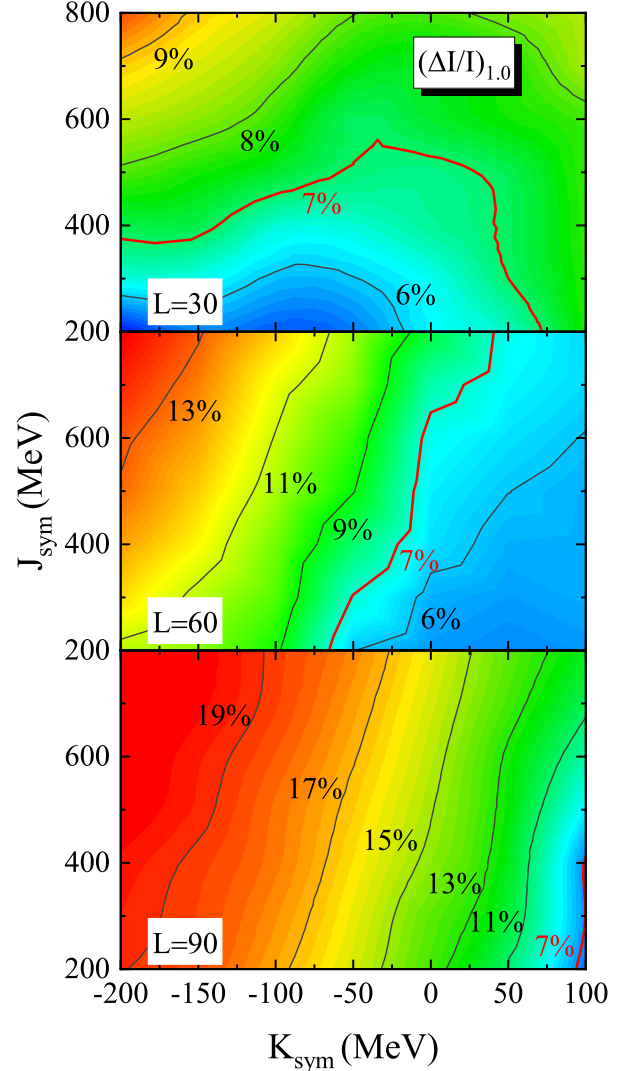


Fig. 3. (color online) The contour of crustal fraction of NS moment of inertia $\Delta I/I$ in the plane of K_{sym} and J_{sym} for the neutron stars with 1.0 M_\odot and slope of symmetry energy $L = 30$ MeV (upper panel), 60 MeV (middle panel), and 90 MeV (lower panel). The red lines indicate the constraint of $\Delta I/I = 7\%$.

Although a neutron star with 1.0 M_\odot can achieve $\Delta I/I \geq 7\%$ for any value of L , we find that: (1) larger J_{sym} is favored for $L = 30$ MeV; (2) smaller K_{sym} is favored for $L = 60$ MeV, while no constraints can be drawn

for J_{sym} ; (3) no constraints can be extracted for K_{sym} and J_{sym} for $L = 90$ MeV. Therefore, the symmetry energy should be treated with caution when calculating the moment of inertia of neutron stars. Additionally, the allowed parameter plane enlarges with L , indicating that a stiffer symmetry energy around saturation density, characterized by L , is more likely to satisfy the constraints imposed by the crustal fraction of NS moment of inertia.

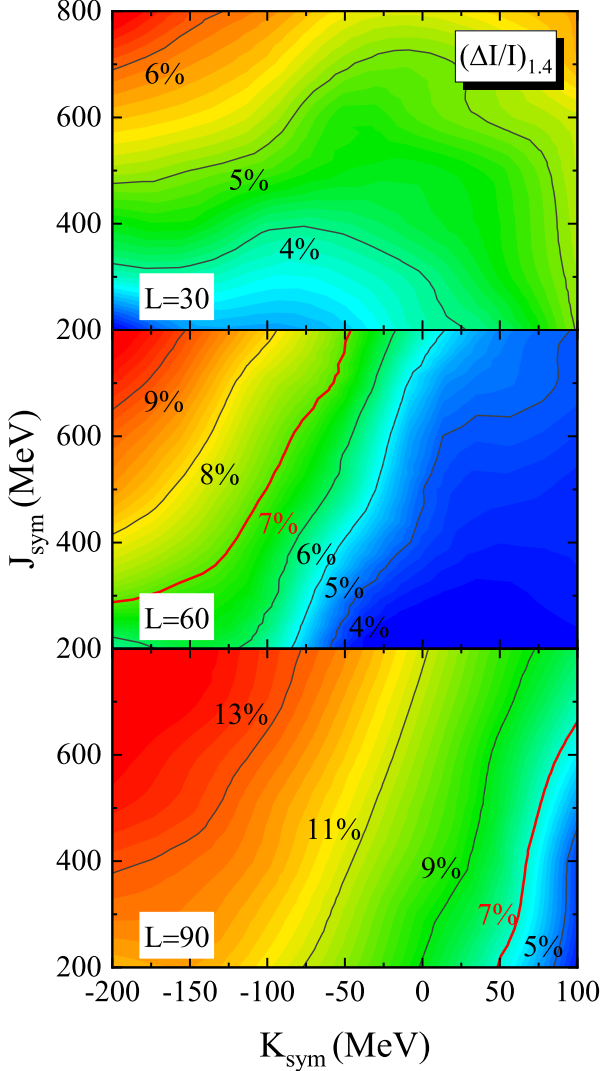


Fig. 4. (color online) Same as Fig. 3 but for neutron stars with $1.4 M_{\odot}$.

For a canonical NS with $M = 1.4 M_{\odot}$, the contours of the crustal fraction of NS moment of inertia $\Delta I/I$ in the K_{sym} versus J_{sym} plane, with $L = 30$ MeV (upper panel), 60 MeV (middle panel), and 90 MeV (lower panel), respectively, are presented in Fig. 4. When compared to Fig. 3, similar features are observed. However, the parameter plane is clearly more tightly constrained for any value of L as the crustal fraction of NS moment of inertia decreases with increasing mass. With $L = 30$

MeV, no parameter combinations can satisfy the constraint $\Delta I/I \geq 7\%$, indicating that this constraint favors a symmetry energy with a larger slope L . For instance, at $L = 60$ MeV, we obtain tighter constraints on K_{sym} and J_{sym} compared to a neutron star with $M = 1.0 M_{\odot}$. The lower limit of J_{sym} is constrained to be 289 MeV, while the upper limit of K_{sym} is constrained to be -46 MeV. This constrained value of K_{sym} is consistent with findings of previous studies that suggest $K_{\text{sym}} = -100 \pm 100$ MeV [20, 49–52]. These constraints on K_{sym} and J_{sym} may indicate a relatively stiff symmetry energy at high densities. For $L = 90$ MeV, the lower right corner of the plane is excluded. However, if the upper limit of K_{sym} is set to 0, the crustal fraction of NS moment of inertia still cannot effectively constrain the symmetry energy.

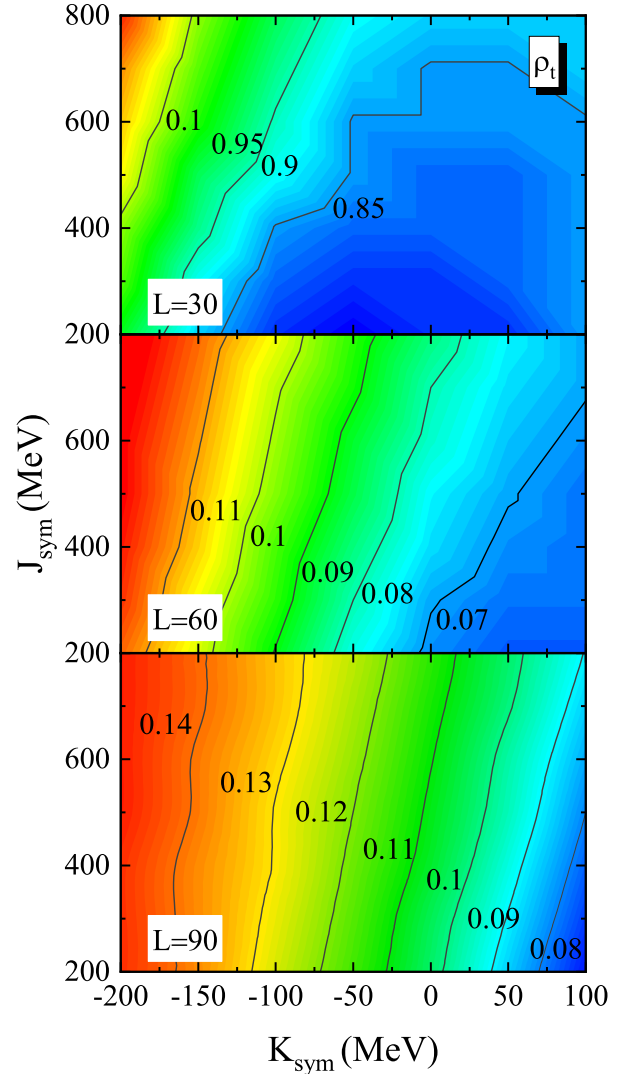


Fig. 5. (color online) The counter of transition density ρ_t in the plane of K_{sym} and J_{sym} .

In summary, the constraint $\Delta I/I \geq 7\%$ does not favor symmetry energies with small slopes (such as $L = 30$

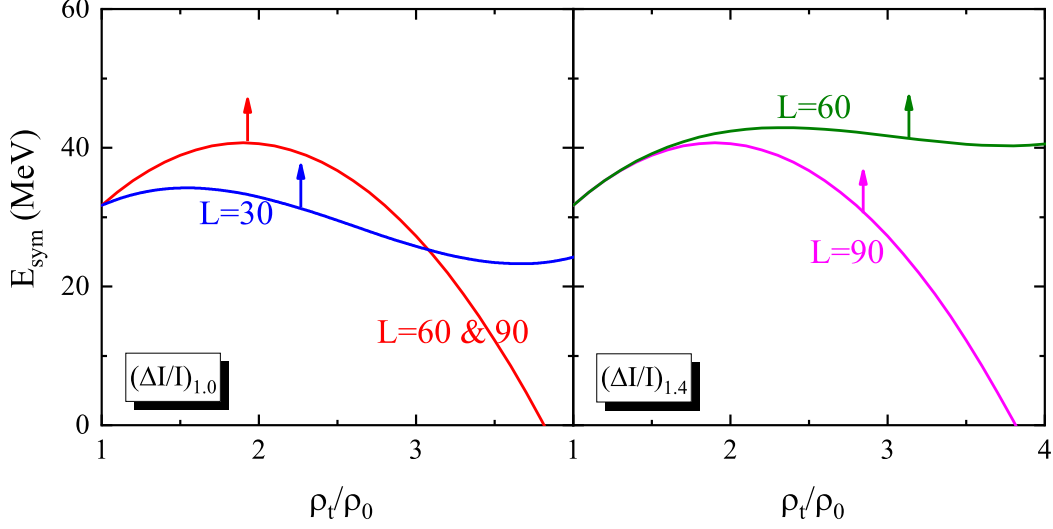


Fig. 6. The lower boundaries of symmetry energy constrained for different slope L of symmetry energy for the neutron stars with $1.0 M_{\odot}$ (left panel) and $1.4 M_{\odot}$ (right panel), respectively.

MeV), and tighter constraints on symmetry energy can be extracted for neutron stars with masses around $1.4 M_{\odot}$. If the neutron star has a significantly larger mass, it is anticipated that only symmetry energies with a considerably larger slope can satisfy this constraint.

The behavior of the constant crustal fraction of NS moment of inertia can be explained through the core-crust transition density and pressure. In Fig. 3 of Ref. [36], we plotted the contours of transition density ρ_t and transition pressure P_t in the L and K_{sym} plane with fixed J_{sym} . We found that, for constant ρ_t , K_{sym} exhibits a monotonic relationship with L when $K_{\text{sym}} < -100$ MeV. However, this relationship becomes more complex for larger values of K_{sym} .

To illustrate effects of J_{sym} on the transition density, we present the contours of transition density ρ_t in the K_{sym} versus J_{sym} plane in Fig. 5. It is evident that the trends for a constant transition density are quite similar to those for a constant moment of inertia shown in Figs. 3 and 4. Notably, the consistency decreases with increasing neutron star mass, which is understandable since the crust of a neutron star is thicker and constitutes a larger mass percentage in lower-mass stars. Consequently, the core-crust transition properties have a more pronounced effect on low-mass neutron stars.

As L , K_{sym} , and J_{sym} are the three parameters characterizing the density dependence of nuclear symmetry energy, the constraints on these parameters can be translated into constraints on the symmetry energy itself. The lower boundaries of the symmetry energy for different slopes L of the symmetry energy, corresponding to neutron stars with $1.0 M_{\odot}$ (left panel) and $1.4 M_{\odot}$ (right panel), are illustrated in Fig. 6. It is important to note that the lower limit of E_{sym} is determined by

the left bottom corner, specifically $K_{\text{sym}} = -200$ MeV and $J_{\text{sym}} = 200$ MeV within the parameter uncertainties, assuming we do not consider the constraints from the crustal fraction of NS moment of inertia. With $L = 60$ and 90 MeV in the case of the neutron star with $1.0 M_{\odot}$, and for $L = 90$ MeV for the neutron star with $1.4 M_{\odot}$, the lower limit of the symmetry energy remains the same, as the left bottom point is not excluded (as shown in Figs. 3 and 4). However, for $L = 30$ MeV for the neutron star with $1.0 M_{\odot}$, J_{sym} cannot be smaller than 294 MeV. Consequently, the symmetry energy along the red line in the upper panel of Fig. 3 can be extracted, and its lower limit is represented as the blue line in the left panel of Fig. 6. Since no parameter combinations can satisfy $\Delta I/I \geq 7\%$ for neutron stars with $1.4 M_{\odot}$ at $L = 30$ MeV, only the lines for $L = 60$ MeV and 90 MeV are plotted in the right panel. Focusing on the blue and green lines, it is clear that the symmetry energy remains nearly constant with increasing density, even for densities $\rho > 3\rho_0$. It is worth noting that the symmetry energy can only be constrained for approximately $\rho < 3\rho_0$ based on the current observations of NSs by NICER [12, 13] and LIGO & Virgo [17] Collaborations, as discussed in our previous study [35]. The present results suggest that the crustal fraction of NS moment of inertia has the potential to constrain the lower limit of the symmetry energy at densities exceeding $3\rho_0$, particularly when L is constrained to values less than 60 MeV.

4 Conclusions

In summary, using an isospin-dependent NS meta-model EOS we investigated the implications of the crustal fraction of NS moment of inertia $\Delta I/I$ for NSs

with $1.0 M_{\odot}$ or $1.4 M_{\odot}$ on the density dependence of nuclear symmetry energy $E_{\text{sym}}(\rho)$. We found that an increase in the slope L and skewness J_{sym} of symmetry energy results in a larger $\Delta I/I$, whereas an increase in the curvature K_{sym} leads to a reduction in $\Delta I/I$. On the other hand, SNM EOS was found to have little influence on the $\Delta I/I$. Our findings highlight the significant role of the symmetry energy parameters in determining the crustal fraction of NS moment of inertia. Moreover, we found that a larger slope L is favored to satisfy the $\Delta I/I \geq 7\%$ constraint, with tighter constraints emerging for neutron stars around $1.4 M_{\odot}$. Fur-

thermore, we extracted the lower boundaries for $E_{\text{sym}}(\rho)$ from the constraint $\Delta I/I \geq 7\%$ for different L values. Our results indicate that the crustal fraction of NS moment of inertia has the potential to set a lower limit of symmetry energy at densities exceeding $3\rho_0$, particularly when L can be constrained to values less than 60 MeV, reflecting the complex interplay between the core-crust transition properties and the underlying nuclear interactions. These findings emphasize the potential of using the crustal fraction of NS moment of inertia to refine our understanding of NS physics and the properties of supradense neutron-rich nuclear matter.

References

- 1 C. Xu and B. A. Li, Phys. Rev. C, **81**: 064612 (2010)
- 2 J. M. Lattimer and M. Prakash, Phys. Rev., **333**: 121 (2020)
- 3 J. M. Lattimer and M. Prakash, Astrophys. J., **550**: 426 (2001)
- 4 P. Danielewicz, R. Lacey, W. G. Lynch, Science, **298**: 1592 (2002)
- 5 J. M. Lattimer, M. Prakash, Phys. Rep., **621**: 127 (2016)
- 6 A. L. Watts, N. Andersson, D. Chakrabarty, et al., Rev. Mod. Phys., **88**: 021001 (2016)
- 7 M. Oertel, M. Hempel, T. Klöhn, and S. Typel, Rev. Mod. Phys., **89**: 015007 (2017)
- 8 F. Özel, P. Freire, Annu. Rev. Astron. Astrophys., **54**: 401 (2016)
- 9 D. Blaschke, N. Chamel, Phases of Dense Matter in Compact Stars, in Astrophysics and Space Science Library, edited by L. Rezzolla, P. Pizzochero, D.I. Jones, N. Rea, I. Vidaña, Astrophysics and Space Science Library, Vol. 457 (Springer, Cham, 2018) p. 337
- 10 H. T. Cromartie *et al.*, Nat. Astron., **4**: 72 (2019)
- 11 E. Fonseca *et al.*, Astrophys. J. Lett., **915**: L12 (2021)
- 12 M. C. Miller *et al.*, Astrophys. J. Lett., **918**: L28 (2021)
- 13 T. E. Riley *et al.*, Astrophys. J. Lett., **918**: L27 (2021)
- 14 T. Salmi *et al.*, Astrophys. J., **941**: 150 (2022)
- 15 T. Salmi, D. Choudhury, Y. Kini, T. E. Riley, S. Vinciguerra, A. L. Watts, M. T. Wolff, Z. Arzoumanian, and S. Bogdanov, Astrophys. J., **974**: 294 (2024)
- 16 A. J. Dittmann, *et al.*, arXiv:2406.14467 (2024)
- 17 B. P. Abbott *et al.*, Phys. Rev. Lett., **121**: 161101 (2018)
- 18 L. Baiotti, Progress in Particle and Nuclear Physics, **109**: 103714 (2019)
- 19 G. F. Burgio, I. Vidana, H. J. Schulze, and J. B. Wei, Progress in Particle and Nuclear Physics, **120**: 103879 (2021)
- 20 B. A. Li, B. J. Cai, W. J. Xie, and N. B. Zhang, Universe, **7**: 182 (2021)
- 21 J. Hooker, W. G. Newton, and B. A. Li, Mon. Not. R. Astron. Soc., **449**: 3559, (2015)
- 22 W. G. Newton, S. Berger, and B. Haskell, Mon. Not. R. Astron. Soc., **454**: 4400 (2015)
- 23 Z. W. Liu, Z. Qian, R. Y. Xing, J. R. Niu, and B. Y. Sun, Phys. Rev. C, **97**: 025801 (2018)
- 24 M. Dutra, C. H. Lenzi, W. de Paula, O. Lourenç, Euro. Phys. J. A, **57**: 260 (2021)
- 25 V. Parmar, H. C. Das, Ankit Kumar, M. K. Sharma, and S. K. Patra, Phys. Rev. D **105**: 043017 (2022)
- 26 V. Radhakrishnan and R. N. Manchester, Nature, **222**: 228 (1969)
- 27 P. E. Reichley and G. S. Downs, Nature, **222**: 229 (1969)
- 28 P. W. Anderson and N. Itoh, Nature, **256**: 25 (1975)
- 29 M. Ruderman, Astrophys. J., **203**: 213 (1976)
- 30 D. Pines and M. A. Alpar, Nature (London), **316**: 27 (1985)
- 31 B. Link, R. I. Epstein, and J. M. Lattimer, Phys. Rev. Lett., **83**: 3362 (1999)
- 32 C. M. Espinoza, A. G. Lyne, B. W. Stappers, and M. Kramer, Mon. Not. R. Astron. Soc., **414**: 1679 (2011)
- 33 N. Andersson, K. Glampedakis, W. C. G. Ho, and C. M. Espinoza, Phys. Rev. Lett., **109**: 241103 (2012)
- 34 N. Chamel, Phys. Rev. C **85**: 035801 (2012)
- 35 N. B. Zhang and B. A. Li, Astrophys. J. **921**: 111 (2021)
- 36 N. B. Zhang, B. A. Li, and J. Xu, Astrophys. J. **859**: 90 (2018)
- 37 J. Oppenheimer and G. Volkoff, Phys. Rev. **55**: 374 (1939)
- 38 I. Bombaci, U. Lombardo, Phys. Rev. C, **44**: 1892 (1991)
- 39 N. B. Zhang and B. A. Li, J. Phys. G: Nucl. Part. Phys., **46**: 014002 (2019)
- 40 N. B. Zhang and B. A. Li, Astrophys. J., **879**: 99 (2019)
- 41 N. B. Zhang and B. A. Li, Astrophys. J., **883**: 61 (2020)
- 42 N. B. Zhang, B. Qi, and S. Y. Wang, Chinese Physics C, **44**: 064103 (2020)
- 43 N. B. Zhang and B. A. Li, Euro. Phys. J. A, **59**: 86 (2023)
- 44 N. B. Zhang and B. A. Li, arXiv:2406.07396 (2024)
- 45 W. J. Xie, B. A. Li, and N. B. Zhang, Phys. Rev. D **110**: 043025 (2024)
- 46 U. Garg and G. Colò, Prog. Part. Nucl. Phys., **101**: 55 (2018)
- 47 S. Shlomo, V. M. Kolomietz, and G. Colò, Euro. Phys. J. A, **30**: 23 (2006)
- 48 B. A. Li and X. Han, Phys. Lett. B, **727**: 276 (2013)
- 49 G. Grams, R. Somasundaram, J. Margueron, and E. Khan, arXiv:2207.01884 (2022)
- 50 J. Margueron, R. H. Casali, and F. Gulminelli, Phys. Rev. C, **97**: 025806 (2018)
- 51 C. Mondal, B. K. Agrawal, J. N. De, S. K. Samaddar, M. Centelles, and X. Viñas, Phys. Rev. C, **96**: 021302 (2017)
- 52 R. Somasundaram, C. Drischler, I. Tews, and J. Margueron, Phys. Rev. C, **103**: 045803 (2021)
- 53 N. B. Zhang and B. A. Li, Euro. Phys. J. A, **55**: 39 (2019)
- 54 W. J. Xie and B. A. Li, Astrophys. J., **883**: 174 (2019)
- 55 W. J. Xie and B. A. Li, Astrophys. J., **899**: 4 (2020)
- 56 B. J. Cai and L. W. Chen, Nucl. Sci. Tech., **28**: 185 (2017)
- 57 N. B. Zhang, B. J. Cai, B. A. Li, W. G. Newton, and J. Xu, Nucl. Sci. Tech., **28**: 181 (2017)
- 58 I. Tews, J. M. Lattimer, A. Ohnishi, and E. E. Kolomeitsev, Astrophys. J., **848**: 105 (2017)
- 59 J. W. Negele and D. Vautherin, Nucl. Phys. A, **207**: 298 (1973)
- 60 G. Baym, C. J. Pethick, and P. Sutherland, Astrophys. J., **170**: 299 (1971)

- 61 R. C. Tolman, PNAS, **20**: 3 (1934)
- 62 S. Kubis, Phys. Rev. C, **70**: 065804 (2004)
- 63 S. Kubis, Phys. Rev. C, **76**: 025801 (2007)
- 64 J. M Lattimer and M. Prakash, Phys. Rep., **442**: 109 (2007)
- 65 J. Xu, L. W. Chen, B. A. Li, and H. R. Ma, Astrophys. J., **697**: 1549 (2009)
- 66 C. Ducoin, J. Margueron, C. Providência, and I. Vidaña, Phys. Rev. C, **83**: 045810 (2011)
- 67 J. Piekarewicz, F. J. Fattoyev, and C. J. Horowitz, Phys. Rev. C, **90**: 015803 (2014)
- 68 T. R. Routray, *et al.*, J. Phys. G: Nucl. Part. Phys., **43**: 105101 (2016)
- 69 A. Worley, P. G. Krastev, and B. A. Li, Astrophys. J., **685**: 390 (2008)
- 70 J. Xu, L. W. Chen, B. A. Li, and H. R. Ma, Phys. Rev. C, **79**: 035802 (2009)